Brinkman penalization Lattice Boltzmann Method simulation of flow past a porous backward-facing step

Léo Roussel [1], Chloé Mimeau [2], Simon Marié [1]

[1]Laboratoire DynFluid, Conservatoire National des Arts et Métiers, Paris

[2]Laboratoire M2N, Conservatoire National des Arts et Métiers, Paris

Examples of flows affected by porous media...

dense barrier

porous barrier

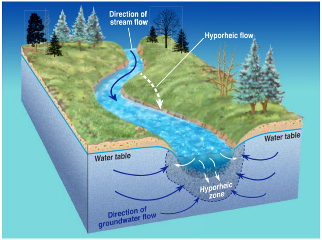

Examples of flows affected by porous media...

dense barrier

porous barrier

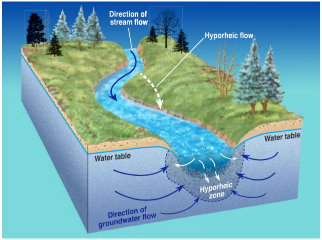

Simulation of fluid-porous flows

- Influence of porous media on a flow involves complex multiscale dynamics;
- But high cost for full resolution at pore scale.

Porous medium model

Porous media characterized by their porosity ϕ_p and Darcy number $\mathrm{Da} = K/L^2$.

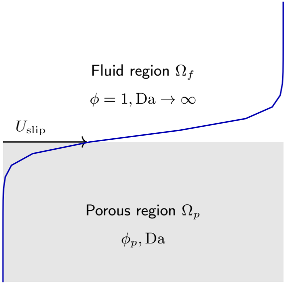

- Incompressible Navier-Stokes equations in Ω_f

$$\frac{\partial \boldsymbol{u}}{\partial t} + (\boldsymbol{u} \cdot \nabla)\boldsymbol{u} = -\nabla p + \frac{1}{\mathrm{Re}} \nabla^2 \boldsymbol{u}.$$

- Brinkman-Darcy-Forchheimer equation in Ω_p

$$0 = -\nabla(\phi_p p) + \frac{1}{\mathrm{Re}} \nabla^2 \boldsymbol{u} - \frac{\phi_p}{\mathrm{ReDa}} \boldsymbol{u} - \frac{\phi_p c_F}{\sqrt{\mathrm{Da}}} |\boldsymbol{u}| \boldsymbol{u}.$$

Porous medium model

Porous media characterized by their porosity ϕ_p and Darcy number $\mathrm{Da} = K/L^2$.

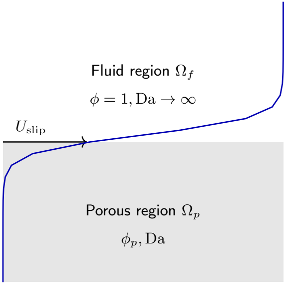

- Incompressible Navier-Stokes equations in Ω_f

$$\frac{\partial \boldsymbol{u}}{\partial t} + (\boldsymbol{u} \cdot \nabla)\boldsymbol{u} = -\nabla p + \frac{1}{\mathrm{Re}} \nabla^2 \boldsymbol{u}.$$

- Brinkman-Darcy-Forchheimer equation in Ω_p

$$0 = -\nabla(\phi_p p) + \frac{1}{\mathrm{Re}} \nabla^2 \boldsymbol{u} - \frac{\phi_p}{\mathrm{ReDa}} \boldsymbol{u} - \frac{\phi_p c_F}{\sqrt{\mathrm{Da}}} |\boldsymbol{u}| \boldsymbol{u}.$$

Brinkman penalization method ($\phi_p \simeq 1$) : single equation in the whole domain

$$\frac{\partial \boldsymbol{u}}{\partial t} + \phi^{-1} (\boldsymbol{u} \cdot \nabla)\boldsymbol{u} = -\nabla(\phi p) + \frac{1}{\mathrm{Re}} \nabla^2 \boldsymbol{u} + \mathbf{F}_p, \quad \phi(\boldsymbol{x}) = \begin{cases} 1, & \boldsymbol{x} \in \Omega_f, \\ \phi_p, & \boldsymbol{x} \in \Omega_p, \end{cases}$$

Penalization term : $\mathbf{F}_p = \mathbb{1}_{\Omega_p} \left(-\frac{\phi_p}{\mathrm{ReDa}} \boldsymbol{u} - \frac{\phi_p c_F}{\sqrt{\mathrm{Da}}} |\boldsymbol{u}| \boldsymbol{u} \right).$

Numerical method

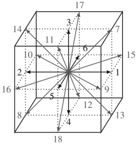

In-house LBM solver : Python-Fortran OpenACC code[1]

$\Longrightarrow$ 74 GLUPS for 48 H100 GPUs on French supercomputer Jean Zay

D3Q19-MRT : $\partial_t f_\alpha + \boldsymbol{c}_\alpha \cdot \nabla_{\boldsymbol{x}} f_\alpha + \mathbf{F}_p \cdot \nabla_{\boldsymbol{c}_\alpha} f_\alpha = \left[\mathbf{M}^{-1}\mathbf{D}\mathbf{M}\boldsymbol{f}\right]_\alpha$.

Implementation of Brinkman penalization in LBM : model of Guo and Zhao, 2002

- Collision : $$\boldsymbol{m}^{\mathrm{coll}}(\boldsymbol{x},t) = \boldsymbol{m}(\boldsymbol{x},t) - \mathbf{D}\left(\boldsymbol{m}(\boldsymbol{x},t) - \boldsymbol{m}^{\mathrm{eq}}(\boldsymbol{x},t)\right) + (\mathbf{I} - \frac{1}{2}\mathbf{D})\mathbf{M}\boldsymbol{S},$$
- Moments : $$\rho = \sum_\alpha f_\alpha,\ \boldsymbol{u} = \sum_\alpha \boldsymbol{c}_\alpha f_\alpha + \frac{\delta_t}{2}\mathbf{F}_p,\ \mathbf{F}_p = \mathbb{1}_{\Omega_p}\left(-\frac{\phi_p}{\mathrm{ReDa}} - \frac{\phi_p c_F}{\sqrt{\mathrm{Da}}}|\boldsymbol{u}|\boldsymbol{u}\right),$$
- Equilibrium : $$f_\alpha^{\mathrm{eq}} = w_\alpha \rho\left(1 + \frac{\boldsymbol{c}_\alpha \cdot \boldsymbol{u}}{c_s^2} + \frac{(\boldsymbol{c}_\alpha \cdot \boldsymbol{u})^2}{2\phi c_s^4} - \frac{|\boldsymbol{u}|^2}{2\phi c_s^2}\right),$$
- Source : $$S_\alpha = w_\alpha\left(\frac{\boldsymbol{c}_\alpha \cdot \mathbf{F}_p}{c_s^2} + \frac{(\boldsymbol{c}_\alpha \cdot \mathbf{F}_p)(\boldsymbol{c}_\alpha \cdot \boldsymbol{u})}{\phi c_s^4} - \frac{\mathbf{F}_p \cdot \boldsymbol{u}}{\phi c_s^2}\right).$$

[1] Junqueira-Junior, C., Medina, E. Z., Taibi, N., & Marié, S. (2026). A python/fortran implementation of the lattice-boltzmann kernel on multiple gpu using the openacc framework. *Concurrency and Computation: Practice and Experience*, *38*(1), e70518.

Prediction of interface velocity U_{slip}

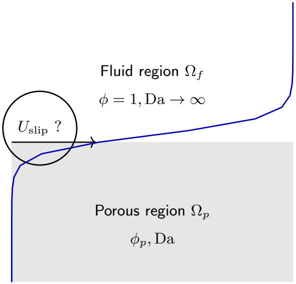

Boundary layer over a porous wall $\longrightarrow$ prediction of interface velocity U_{slip} ?

Prediction of interface velocity U_{slip}

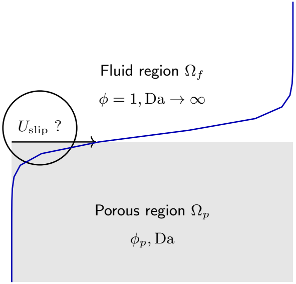

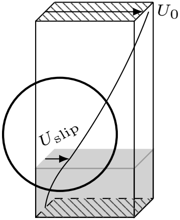

Boundary layer over a porous wall $\longrightarrow$ prediction of interface velocity U_{slip} ?

Prediction of interface velocity U_{slip}

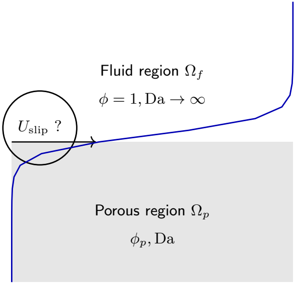

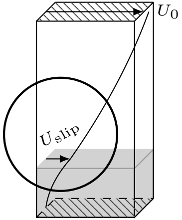

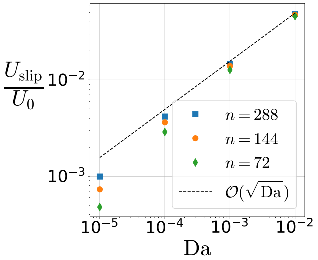

Boundary layer over a porous wall $\longrightarrow$ prediction of interface velocity U_{slip} ?

Comparison to the asymptotic solution of the Brinkman penalization equation (Carbou and Fabrie, 2003) $\implies$ faster convergence of U_{slip} for increasing Da

Mimeau, C., Marié, S., Roussel, L., & Mortazavi, I. (2024).Wake prediction in 3d porous–fluid flows: A numerical study using a brinkman penalization lbm approach. *Flow, Turbulence and Combustion*, *112*(1), 273–301. https://doi.org/10.1007/s10494-023-00471-w.

Application to the porous step : numerical setup

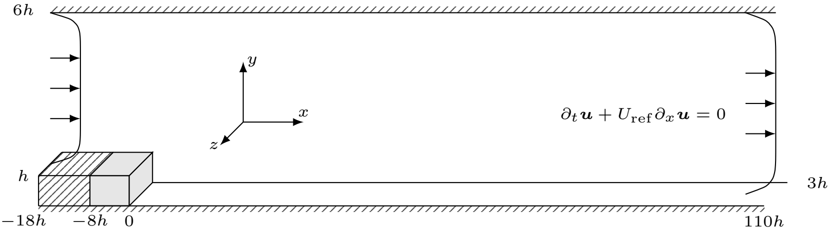

- Permeability $\mathrm{Da} \equiv K/h^2 = \mathbf{0}$ **(solid)**, $\underbrace{6.8 \times 10^{-4}}_{\text{weakly permeable}}$, $\underbrace{3.3 \times 10^{-3}}_{\text{highly permeable}}$.
- $\mathrm{Re} \equiv U_0 h/\nu = 350,\ 510,\ 700.$
- Boundary conditions : non-equilibrium finite-difference method (Latt et al., 2008)

$$f_\alpha(\boldsymbol{x}, t) = f_\alpha^{\mathrm{eq}}(\rho, \boldsymbol{u}) + f_\alpha^{\mathrm{neq}}(\nabla \boldsymbol{u}) = f_\alpha^{\mathrm{eq}}(\rho, \boldsymbol{u}) - \frac{\rho \tau_\nu w_\alpha}{c_s^2} \nabla \boldsymbol{u} : (\boldsymbol{c}_\alpha \boldsymbol{c}_\alpha - c_s^2 \mathbf{I}).$$

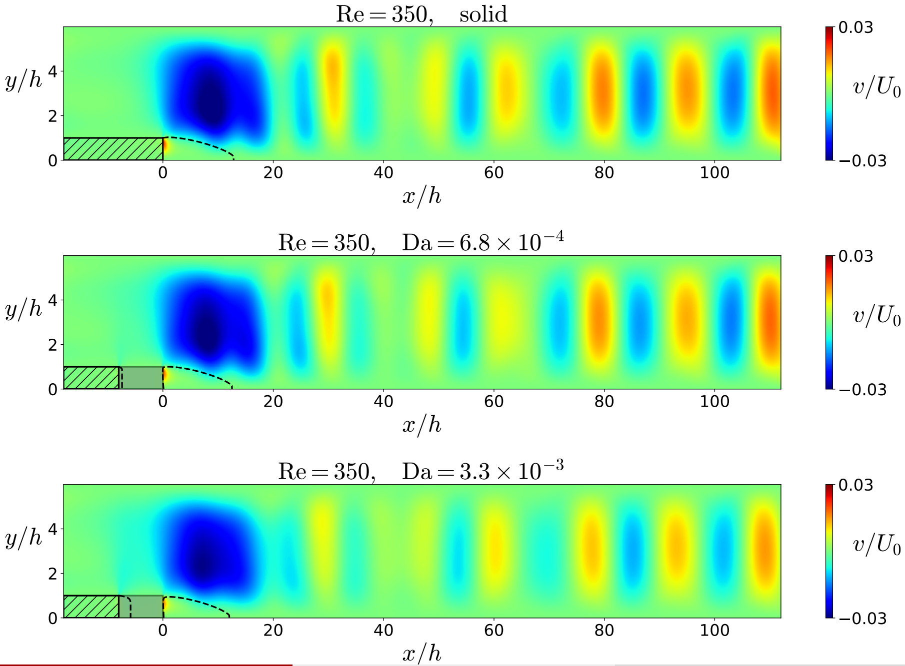
$\mathrm{Re} = 350$, solid
$\mathrm{Re} = 350$, $\mathrm{Da} = 6.8 \times 10^{-4}$
$\mathrm{Re} = 350$, $\mathrm{Da} = 3.3 \times 10^{-3}$
y/h
0
2
4
x/h
0
20
40
60
80
100
v/U_0
0.03
−0.03

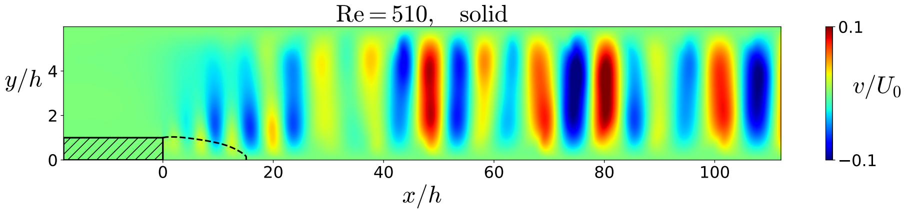
$\mathrm{Re} = 510$, solid
y/h
x/h
0
2
4
0
20
40
60
80
100
0.1
−0.1
v/U_0

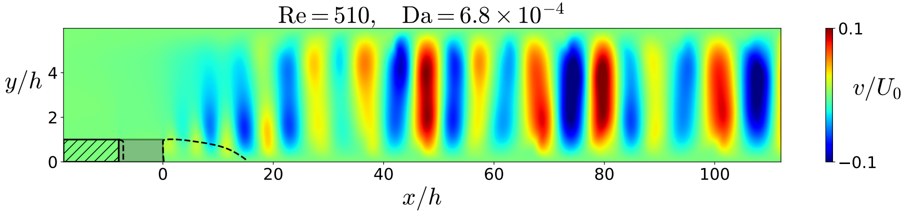
$\mathrm{Re} = 510$, $\mathrm{Da} = 6.8 \times 10^{-4}$
y/h
x/h
0
2
4
0
20
40
60
80
100
0.1
−0.1
v/U_0

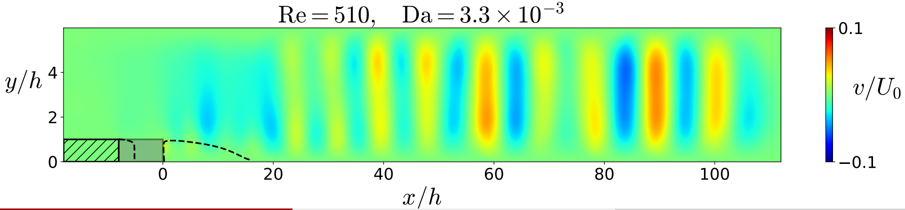
$\mathrm{Re} = 510$, $\mathrm{Da} = 3.3 \times 10^{-3}$
y/h
x/h
0
2
4
0
20
40
60
80
100
0.1
−0.1
v/U_0

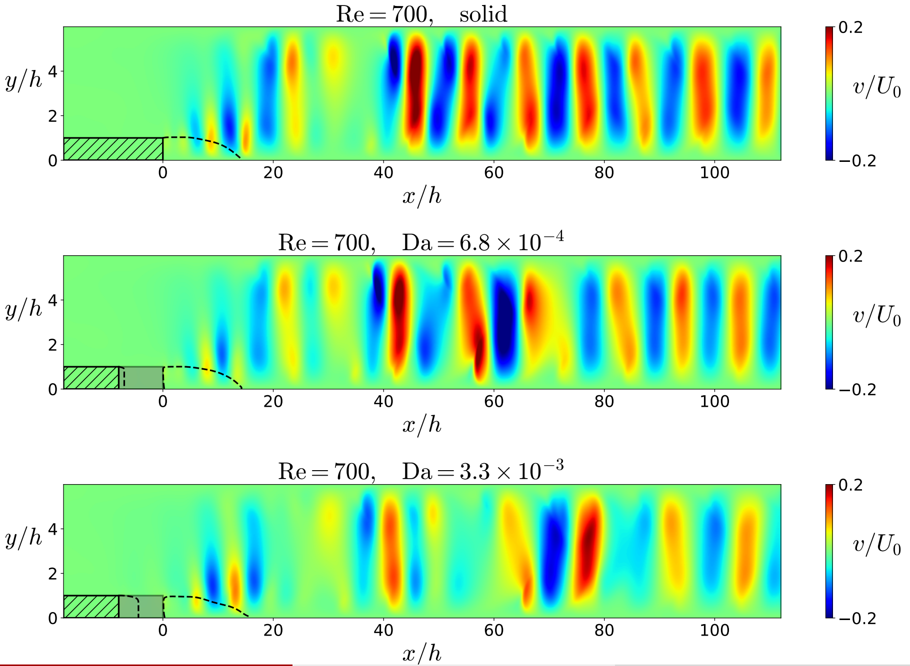
$\mathrm{Re} = 700$, solid
$\mathrm{Re} = 700$, $\mathrm{Da} = 6.8 \times 10^{-4}$
$\mathrm{Re} = 700$, $\mathrm{Da} = 3.3 \times 10^{-3}$
y/h
x/h
v/U_0
0.2
−0.2
0
2
4
20
40
60
80
100

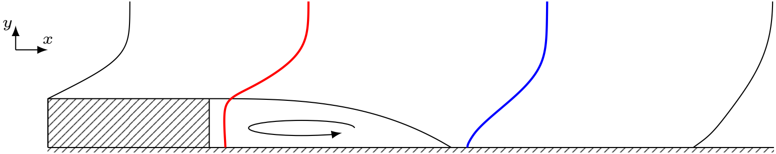

Solid backward-facing step : frequency signatures

- High-frequency Kelvin-Helmholtz instability of the shear layer at separation;
- Low-frequency Tollmien-Schlichting instability of the reattached boundary layer.

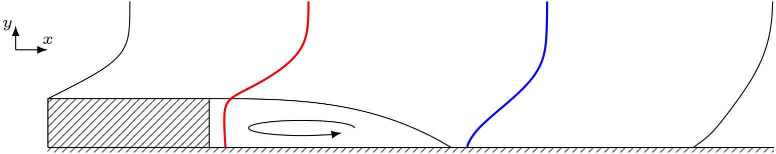

Solid backward-facing step : frequency signatures

- High-frequency Kelvin-Helmholtz instability of the shear layer at separation;
- Low-frequency Tollmien-Schlichting instability of the reattached boundary layer.

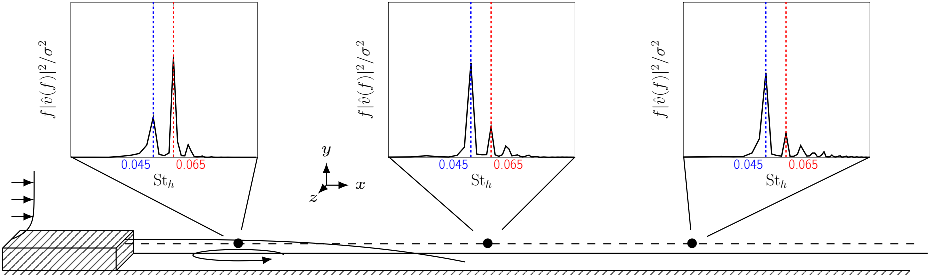

$\mathrm{Re} = 350$

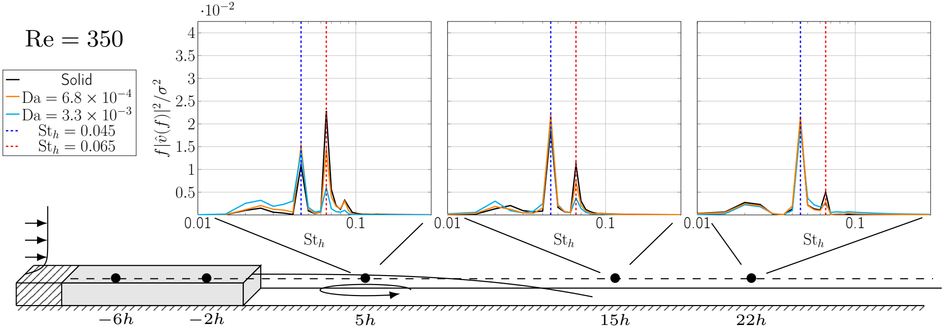

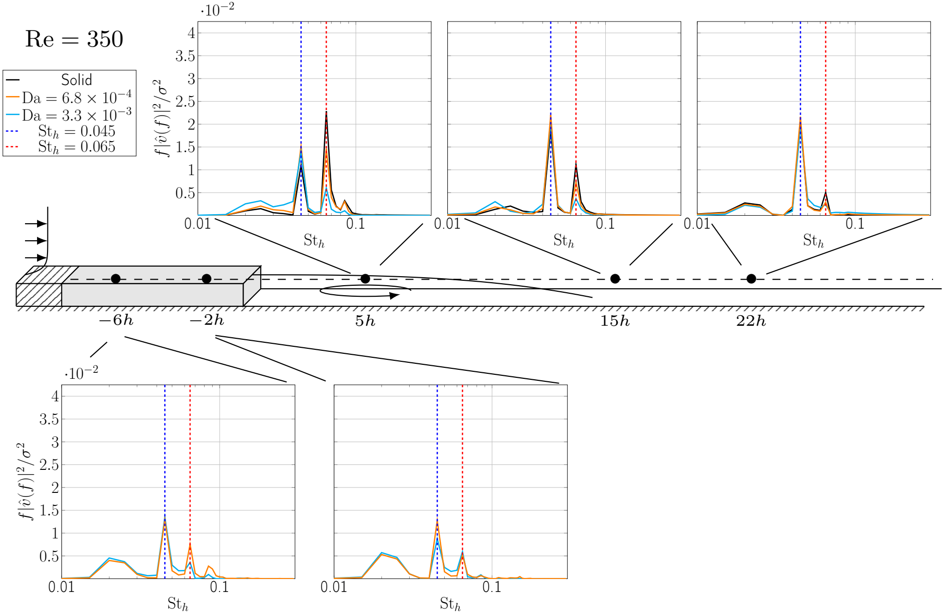

Re = 350
Solid
Da = 6.8 × 10^−4
Da = 3.3 × 10^−3
St_h = 0.045
St_h = 0.065
·10^−2
f|v̂(f)|²/σ²
St_h
0.01
0.1
−6h
−2h
5h
15h
22h

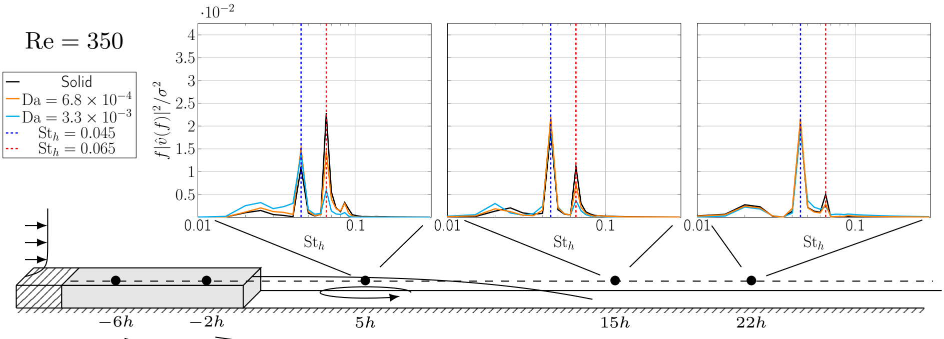

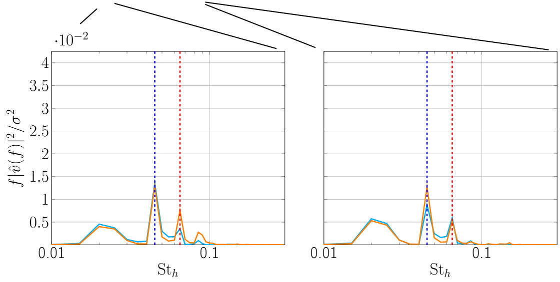

- High frequency $\mathrm{St} = 0.065$ attenuated by the porous steps.
- Dominant low-frequency peak $\mathrm{St} = 0.045$ at all stations.
- Presence of a very low frequency $\mathrm{St}_h = 0.02$.

$\mathrm{Re} = 510$

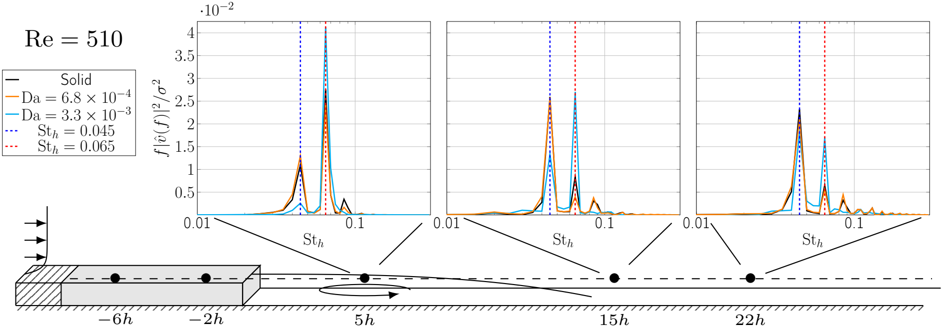

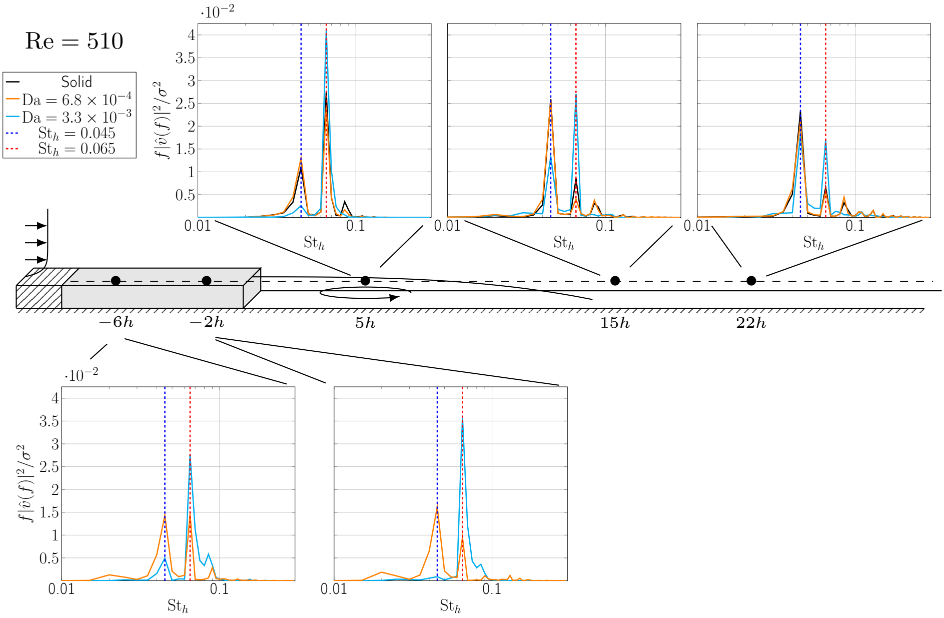
Re = 510
Solid
Da = 6.8 × 10^−4
Da = 3.3 × 10^−3
St_h = 0.045
St_h = 0.065
·10^−2
f|v̂(f)|²/σ²
St_h
0.01
0.1
−6h
−2h
5h
15h
22h

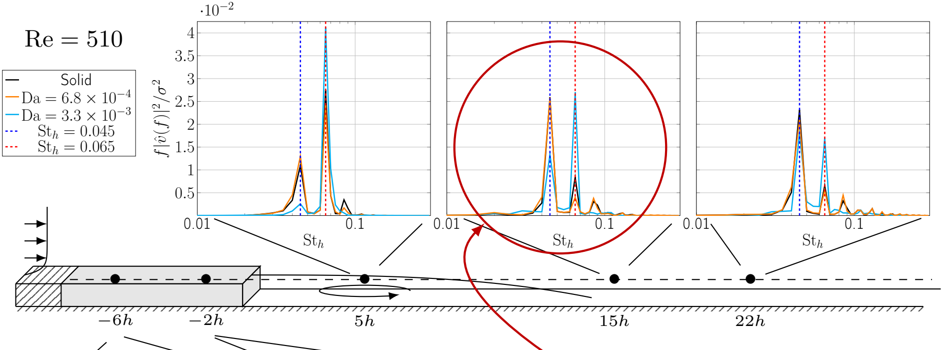

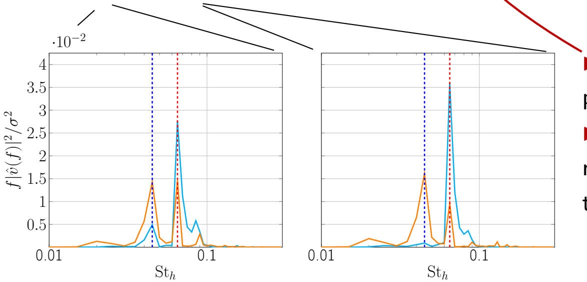

- Frequency cross-over for high permeability $\mathrm{Da} = 3.3 \times 10^{-3}$.
- Dynamics inside the porous medium shows similar trends to that past the step.

$\mathrm{Re} = 700$

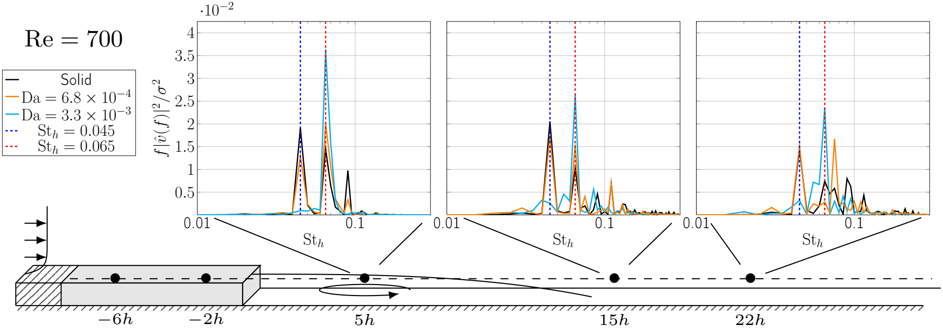

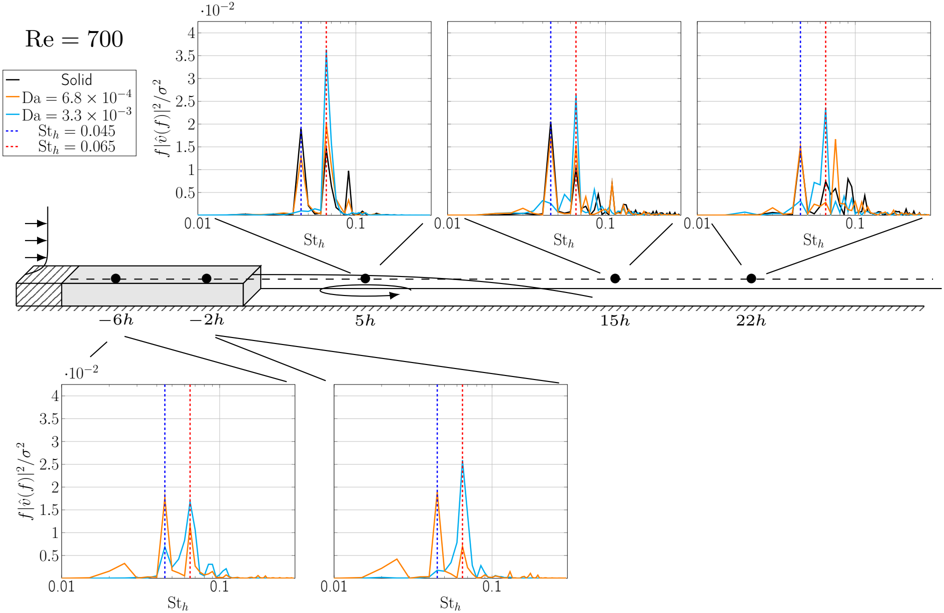
Re = 700
Solid
Da = 6.8 × 10^−4
Da = 3.3 × 10^−3
St_h = 0.045
St_h = 0.065
·10^−2
f|v̂(f)|²/σ²
0.5
1
1.5
2
2.5
3
3.5
4
0.01
0.1
St_h
−6h
−2h
5h
15h
22h

$\mathrm{Re} = 700$

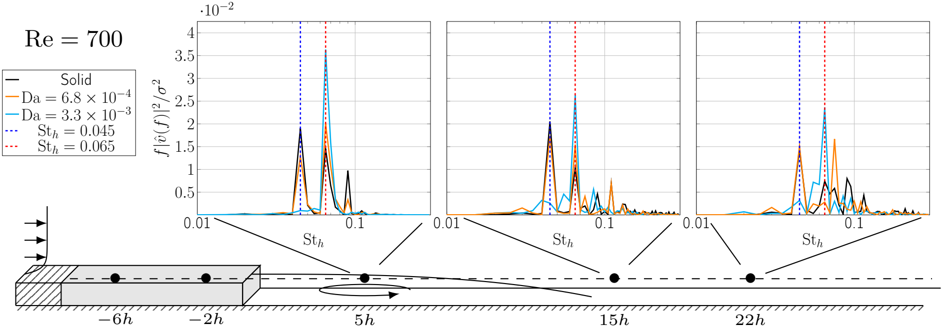

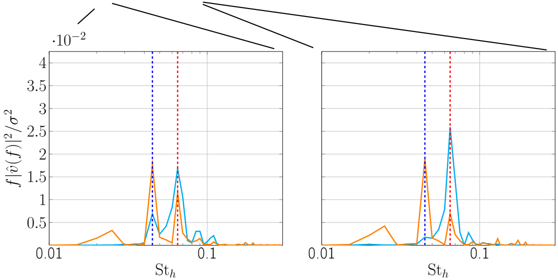

- Kelvin-Helmholtz frequency $\mathrm{St}_h = 0.065$ globally dominant for $\mathrm{Da} = 3.3 \times 10^{-3}$.
- Onset of frequency cross-over at $\mathrm{Da} = 6.8 \times 10^{-4}$?

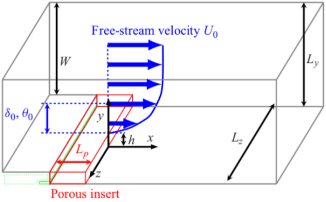

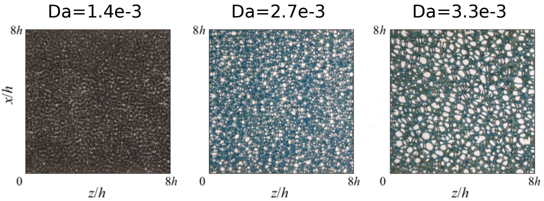

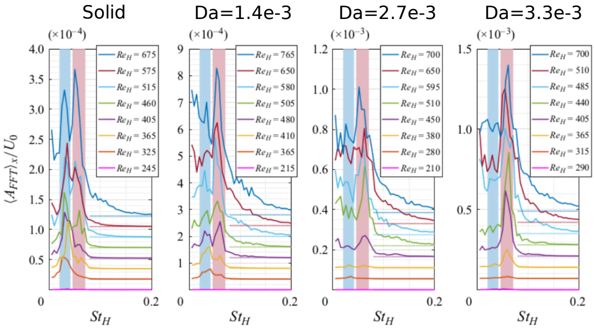

Porous step experiment by Klotz et al., 2024[2]

$\implies$ critical Reynolds number of the frequency cross-over decreases as the permeability of the step increases.

[2] Klotz, L., Bukowski, K., & Gumowski, K. (2024). Influence of porous material on the flow behind a backward-facing step: Experimental study. *Journal of Fluid Mechanics, 998.* https://doi.org/10.1017/jfm.2024.639.

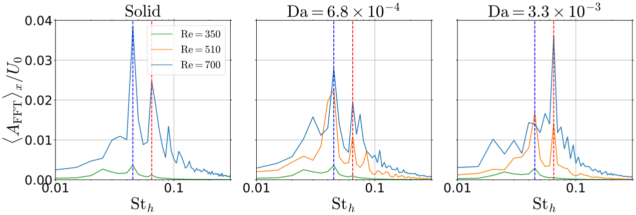

Frequency cross-over phenomenon observed for the highly permeable step at $\mathrm{Da} = 3.3 \times 10^{-3}$.

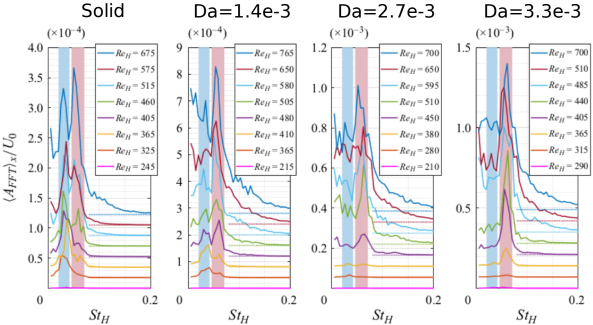

Porous step experiment by Klotz et al., 2024[2]

$\Longrightarrow$ critical Reynolds number of the frequency cross-over decreases as the permeability of the step increases.

[2] Klotz, L., Bukowski, K., & Gumowski, K. (2024). Influence of porous material on the flow behind a backward-facing step: Experimental study. *Journal of Fluid Mechanics, 998*. https://doi.org/10.1017/jfm.2024.639.

Turbulent flow at $\mathrm{Re} = 5100$

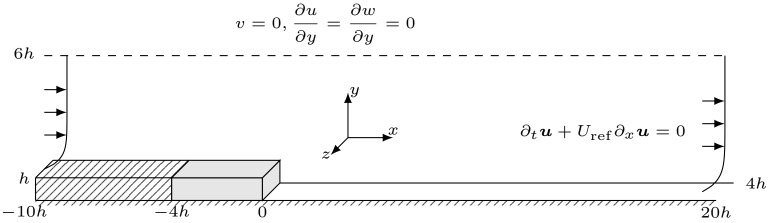

- DNS with $\Delta x_i^+ \simeq 1.2$ upstream of the step edge;
- Synthetic turbulence generation with the Random Fourier Modes method;
- Free-slip condition at the top boundary;
- Solid step reference case and porous step with $\mathrm{Da} = 3.3 \times 10^{-3}$.

Turbulent flow at $\mathrm{Re} = 5100$

Iso-surfaces of λ_2-criterion colored by velocity norm

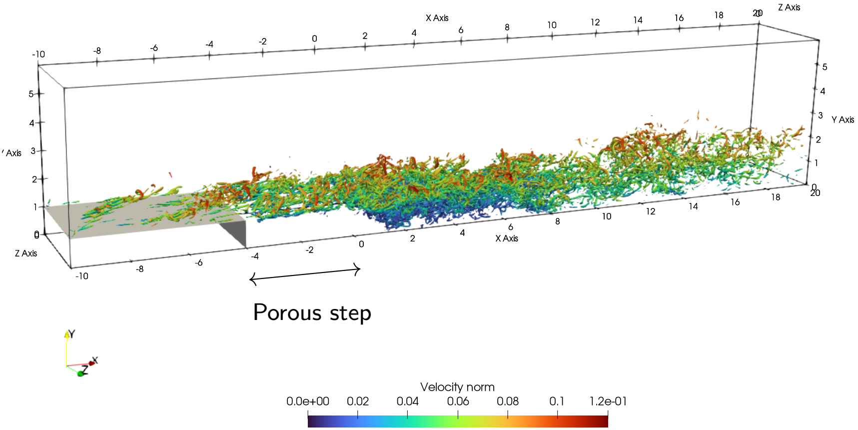

Porous step

Turbulent flow at $\mathrm{Re} = 5100$

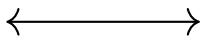

Turbulent flow at $\mathrm{Re} = 5100$

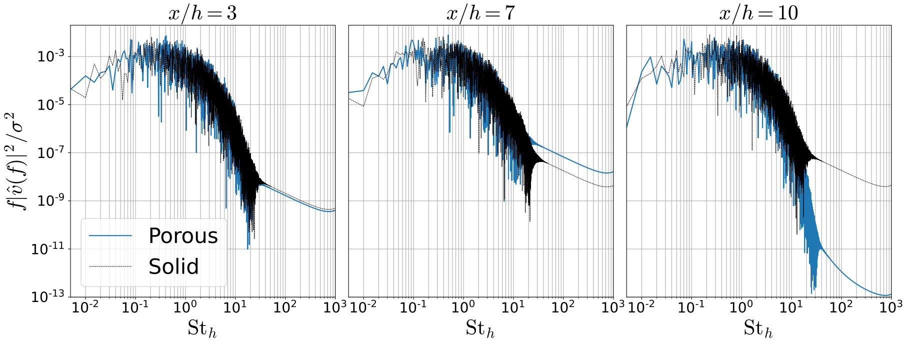

- Laminar unsteady flow at $\mathrm{Re} = 350,\ 510,\ 700$
  - First Brinkman penalization LBM study of the porous BFS (no dedicated interface treatment);
  - Qualitative agreement with experimental results of Klotz *et al.* 2024[3]: frequency cross-over phenomenom for large Da.
- Turbulent flow at $\mathrm{Re} = 5100$: amplification of the Kelvin-Helmholtz instability
- Perspectives : turbulence modelling in porous media ?

Carbou, G., & Fabrie, P. (2003).Boundary layer for a penalization method for viscous incompressible flow. *Advances in Differential Equations*, *8*(12), 1453–1480. https://doi.org/10.57262/ade/1355867981

Guo, Z., & Zhao, T. S. (2002).Lattice boltzmann model for incompressible flows through porous media. *Phys. Rev. E*, *66*, 036304. https://doi.org/10.1103/PhysRevE.66.036304

Junqueira-Junior, C., Medina, E. Z., Taibi, N., & Marié, S. (2026).A python/fortran implementation of the lattice-boltzmann kernel on multiple gpu using the openacc framework. *Concurrency and Computation: Practice and Experience*, *38*(1), e70518.

Klotz, L., Bukowski, K., & Gumowski, K. (2024).Influence of porous material on the flow behind a backward-facing step: Experimental study. *Journal of Fluid Mechanics*, *998*. https://doi.org/10.1017/jfm.2024.639

Latt, J., Chopard, B., Malaspinas, O., Deville, M., & Michler, A. (2008).Straight velocity boundaries in the lattice boltzmann method. *Phys. Rev. E*, *77*, 056703. https://doi.org/10.1103/PhysRevE.77.056703

Mimeau, C., Marié, S., Roussel, L., & Mortazavi, I. (2024).Wake prediction in 3d porous–fluid flows: A numerical study using a brinkman penalization lbm approach. *Flow, Turbulence and Combustion*, *112*(1), 273–301.